

# Modelling Collective Cell Behaviour in Repair and Disease

Philip K. Maini

Wolfson Centre for Mathematical Biology

Mathematical Institute, Oxford

[maini@maths.ox.ac.uk](mailto:maini@maths.ox.ac.uk)

# Outline

- (1) Angiogenesis – the formation of new blood vessels**
- (2) Cancer Cell Invasion**

# ANGIOGENESIS

# Angiogenesis

- In wound healing/cancer growth, new blood vessels form by endothelial cells escaping from existing blood vessels and moving towards the wound/tumour – this is termed *angiogenesis*
- There are many very sophisticated models now for angiogenesis.

Our aim in this talk is to take inspiration from the simplest model and ask the more general question:  
**If we propose rules of behaviour at the cell level – how do we scale up to the tissue level?**

# Schematic

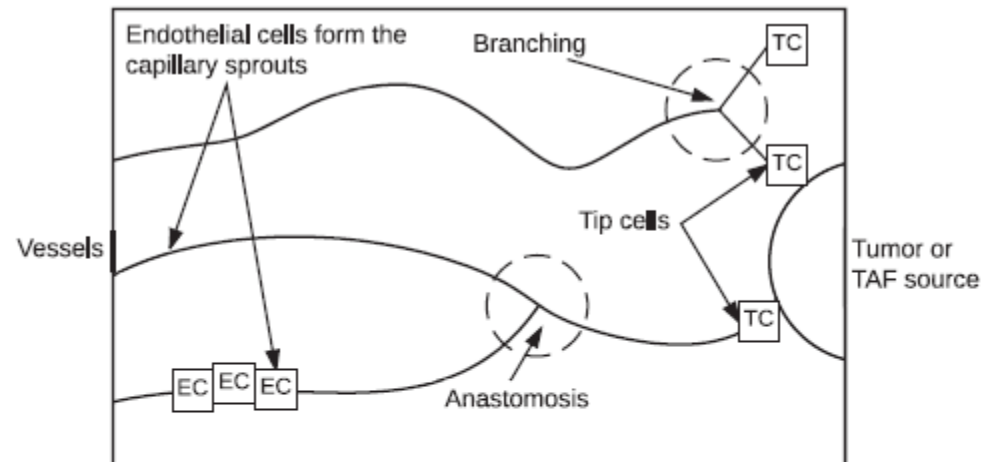
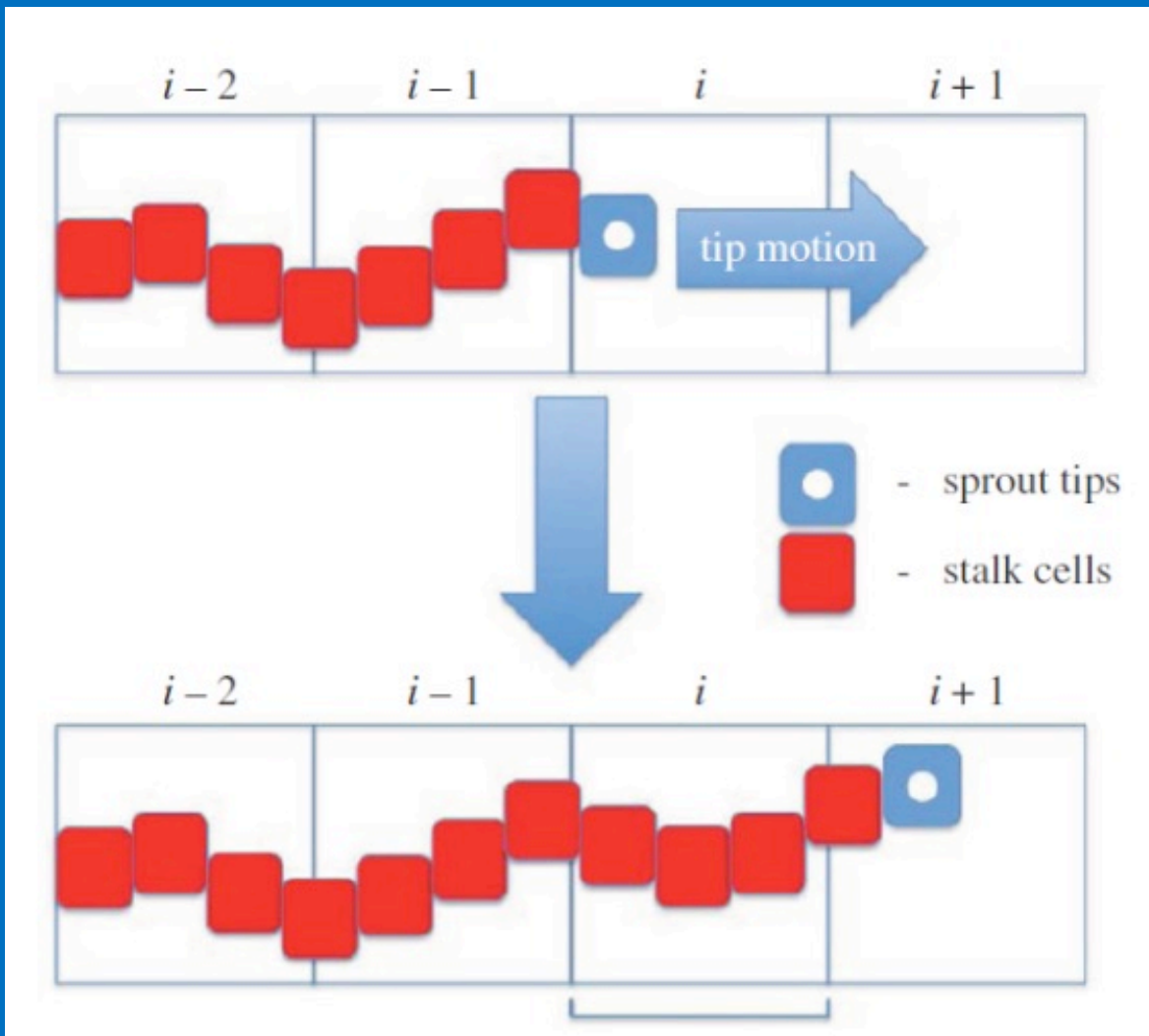


FIG. 1. A schematic of angiogenesis. Endothelial cells follow the paths of tip cells, which move chemotactically in response to a tumor angiogenic factor (TAF) source to form sprouts. Sprouts may branch and fuse through anastomosis to form loops. EC = endothelial cell, TC = tip cell.

# Snail-trail model



Balding D, McElwain D. 1985 A mathematical model of tumour-induced capillary growth. *J. Theor. Biol.* **114**, 53–73. (doi:10.1016/S0022-5193(85)80255-1)  
Byrne HM, Chaplain MAJ. 1996 Explicit solutions of a simplified model of capillary sprout growth during tumor angiogenesis. *Appl. Math. Lett.* **9**, 69–74. (doi:10.1016/0893-9659(95)00105-0)

# The snail-trail model

- Let  $n(x,t)$  be tip cell density and  $e(x,t)$  be endothelial (sprout) cell density

$$\frac{\partial n}{\partial t} = D\nabla^2 n - \chi \nabla \cdot (n \nabla c) + \lambda n c - \beta_e n e - \beta_n n^2,$$
$$\frac{\partial e}{\partial t} = \frac{\kappa(x, y)}{h} \|\chi n \nabla c - D \nabla n\|_2.$$

H. M. Byrne and M. A. J. Chaplain, *Bull. Math. Biol.* **57**, 461 (1995).

F. Spill, P. Guerrero, T. Alarcón, P. K. Maini, and H. M. Byrne, *J. Math. Biol.* **70**, 485 (2015).

Edelstein L (1982) The propagation of fungal colonies: a model for tissue growth. *J Theor Biol* 98(4):679–701

D. Balding and D. L. S. McElwain, *J. Theor. Biol.* **114**, 53 (1985).



# Aside: Scaling Factor

- Martinson, Byrne, Maini, Evaluating snail-trail frameworks for leader-follower behaviour with agent-based modelling, *Phys Rev. E.* 102, 062417 (2020)

$$\frac{\partial n}{\partial t} = D\nabla^2 n - \chi \nabla \cdot (n \nabla c) + \lambda n c - \beta_e n e - \beta_n n^2,$$

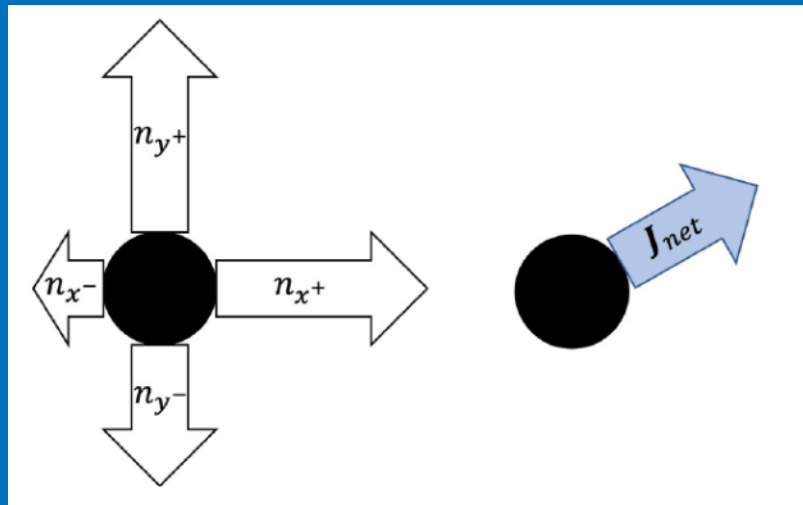
$$\frac{\partial e}{\partial t} = \frac{\kappa(x, y)}{h} \|\chi n \nabla c - D \nabla n\|_2.$$

$$P(X_R = m) = \binom{\kappa}{m} (P_{x^+})^m (1 - P_{x^+})^{\kappa - m},$$

$$\mathbb{E}[X_R] = \kappa P_{x^+}, \quad \mathbb{E}[X_L] = \kappa P_{x^-},$$

$$\mathbb{E}[Y_U] = \kappa P_{y^+}, \quad \mathbb{E}[Y_D] = \kappa P_{y^-},$$

$$\kappa(x, y) \approx \frac{1}{kh \|\nabla c(x, y)\|_2},$$



R. D. M. Travasso, E. C. Poiré, M. Castro, J. C. Rodriguez-Manzaneque, and A. Hernández-Machado, *PLoS ONE* 6, e19989 (2011).

G. Vilanova, I. Colominas, and H. Gomez, *Comput. Mech.* 53, 449 (2014).

- What the above model does is take what is happening to a cell and assume that the population behaves in the same way.
- We follow an alternative procedure:
- (i) We take a square lattice
- (ii) Incorporate the rules on updating lattice occupancy at the cell level
- (iii) Coarse-grain and arrive at a continuum model

S. Pillay, H. M. Byrne, and P. K. Maini, *J. Math. Biol.* **77**, 1721 (2018).

S. Pillay, H. M. Byrne, and P. K. Maini, *Phys. Rev. E* **95**, 012410 (2017).

# The chemoattractant Vascular Endothelial Growth Factor (VEGF)

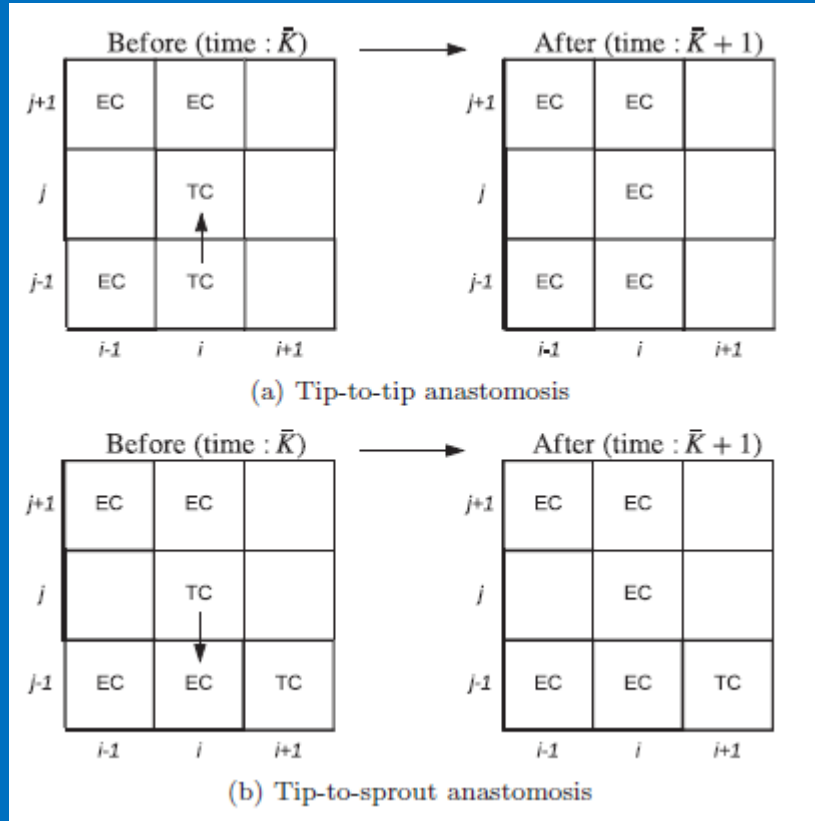
$$c(x, y) = x.$$

# Biased random walk for tip cells

$$P_{x\pm}(i, j) = \frac{1 \pm g_x(i, j)}{4}, \quad 0 < i, j < R,$$
$$P_{y\pm}(i, j) = \frac{1 \pm g_y(i, j)}{4}, \quad 0 < i, j < R,$$

$$g_x(i, j) = k (c_{i+1, j} - c_{i-1, j}), \quad 0 < i, j < R,$$
$$g_y(i, j) = k (c_{i, j+1} - c_{i, j-1}), \quad 0 < i, j < R,$$

# Anastomosis (tip-to-tip or tip-sprout)

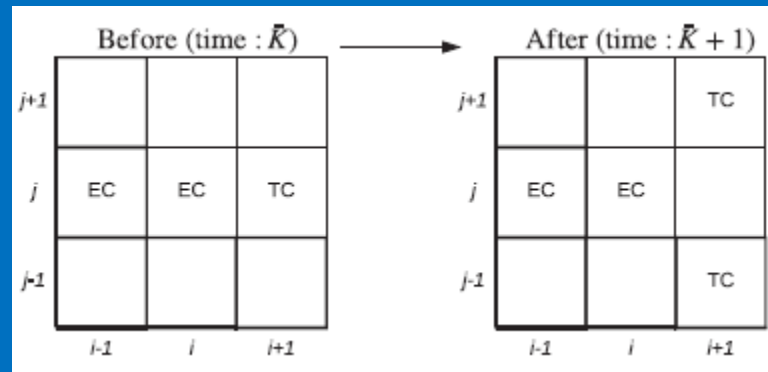


$TC + TC \rightarrow EC$

$TC + EC \rightarrow EC$

# Branching

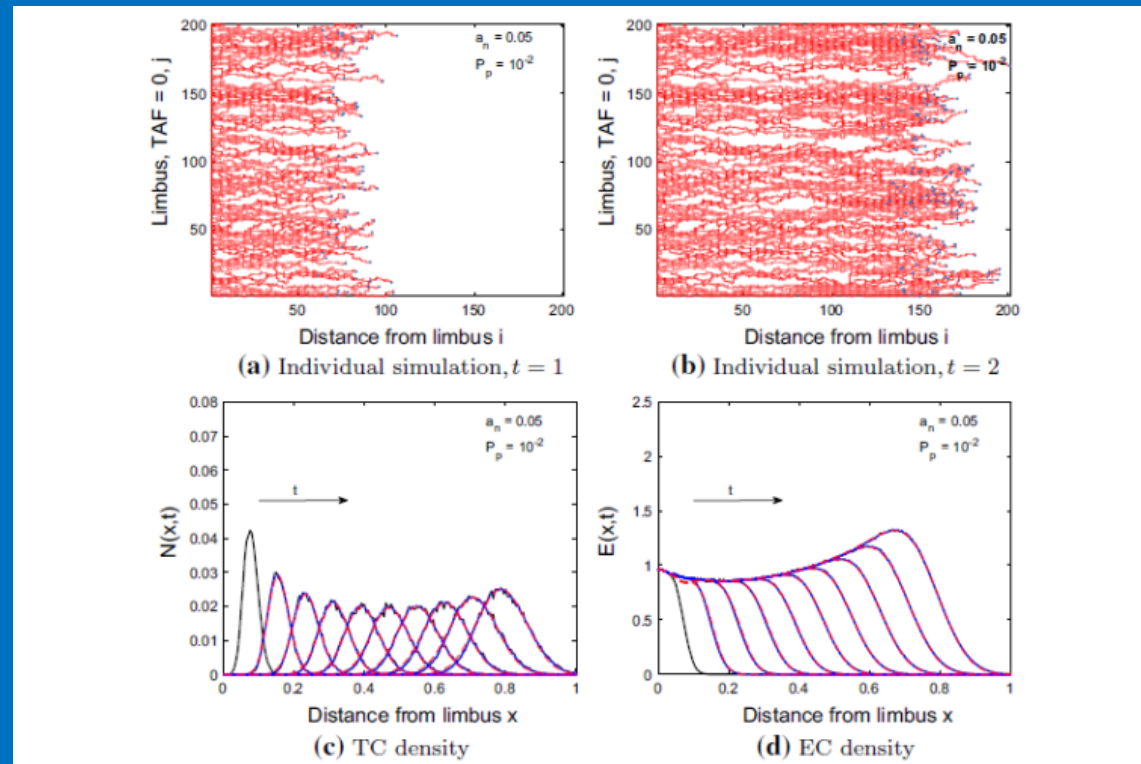
Perpendicular to direction of motion



$$P_b(i, j) = P_p c_{i, j} \in [0, 1]$$

# Comparison of agent-based model with Snail-Trail Model

- S. Pillay, H.M. Byrne, P.K. Maini, The impact of exclusion processes on angiogenesis models, J. Math. Biol., 77, 1721-1759 (2018)



# Ensemble Averages

$$n_{i,j}(\bar{K}) = \frac{1}{M} \sum_{m=1}^M n_{i,j}^m(\bar{K}), \quad e_{i,j}(\bar{K}) = \frac{1}{M} \sum_{m=1}^M e_{i,j}^m(\bar{K}),$$

- Do M realisations then average the occupancies

$$\delta n_{i,j} = n_{i,j}(\bar{K} + 1) - n_{i,j}(\bar{K}),$$

$$\delta e_{i,j} = e_{i,j}(\bar{K} + 1) - e_{i,j}(\bar{K}),$$



$$\begin{aligned}
\delta n_{i,j} = P_m & \left\{ \underbrace{P_{x+}(i-1,j)n_{i-1,j} + P_{x-}(i+1,j)n_{i+1,j} + P_{y+}(i,j-1)n_{i,j-1} + P_{y-}(i,j+1)n_{i,j+1}}}_{\text{movement into } (i,j)} \right. \\
& - \underbrace{[P_{x+}(i,j) + P_{x-}(i,j) + P_{y+}(i,j) + P_{y-}(i,j)]n_{i,j}}_{\text{movement out of } (i,j)} \\
& - \underbrace{a_n n_{i,j} [P_{x+}(i-1,j)n_{i-1,j} + P_{x-}(i+1,j)n_{i+1,j} + P_{y+}(i,j-1)n_{i,j-1} + P_{y-}(i,j+1)n_{i,j+1}]}_{\text{tip-to-tip anastomosis}} \\
& \left. - \underbrace{a_e e_{i,j} [P_{x+}(i-1,j)n_{i-1,j} + P_{x-}(i+1,j)n_{i+1,j} + P_{y+}(i,j-1)n_{i,j-1} + P_{y-}(i,j+1)n_{i,j+1}]}_{\text{tip-to-sprout anastomosis}} \right\} \\
& + \underbrace{P_p c_{i,j} (n_{i,j-1} + n_{i,j+1} - n_{i,j})}_{\text{branching}}
\end{aligned}$$

We introduce two binary variables,  $a_n$  and  $a_e$ , to act as switches for tip-to-tip and tip-to-sprout anastomosis, respectively. If these variables are set to 1, then the corresponding anastomosis process is active.

# continued

$$\delta e_{i,j} = P_m \left\{ \underbrace{P_{x+}(i,j) + P_{x-}(i,j) + P_{y+}(i,j) + P_{y-}(i,j)}_{\text{movement of TCs out of } (i,j)} \right. \\ \left. + a_n \underbrace{[P_{x+}(i-1,j)n_{i-1,j} + P_{x-}(i+1,j)n_{i+1,j} + P_{y+}(i,j-1)n_{i,j-1} + P_{y-}(i,j+1)n_{i,j+1}]}_{\text{tip-to-tip anastomosis}} \right\} n_{i,j}$$

# Discrete to continuum

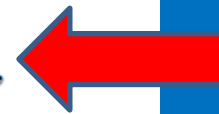
$$\frac{\partial n}{\partial t} = (1 - a_n n - a_e e)[D \nabla^2 n - \chi \nabla \cdot (n \nabla c)] - \mu(a_n n^2 + a_e n e) + c \left( \lambda n + D_b \frac{\partial^2 n}{\partial y^2} \right)$$

and

$$\frac{\partial e}{\partial t} = \mu n + a_n n [\mu n + D \nabla^2 n - \chi \nabla \cdot (n \nabla c)],$$

respectively, where

$$\mu = \lim_{\tau \rightarrow 0} \frac{P_m}{\tau}, \quad \lambda = \lim_{\tau \rightarrow 0} \frac{P_p}{\tau},$$



$$D = \frac{\mu h^2}{4} = \lim_{\tau \rightarrow 0} \frac{P_m h^2}{4\tau}, \quad \chi = \mu k h^2 = \lim_{\tau \rightarrow 0} \frac{P_m k h^2}{\tau}$$

$$D_b = \lambda h^2 = \lim_{\tau \rightarrow 0} \frac{P_p h^2}{\tau}.$$



M. J. Simpson, K. A. Landman, and B. D. Hughes, *Phys. Rev. E* (Amsterdam, Neth.) **389**, 3779 (2010).

M. J. Simpson, K. A. Landman, and B. D. Hughes, *Phys. Rev. E* (Amsterdam, Neth.) **388**, 399 (2009).

E. A. Codling, M. J. Plank, and S. Benhamou, *J. R. Soc. Interface* **5**, 813 (2008).

# Boundary and initial conditions

$$D \frac{\partial n}{\partial x} - \chi n \frac{\partial c}{\partial x} = 0, \quad \text{at } x = 0, 1, \quad 0 \leq y \leq 1,$$
$$D \frac{\partial n}{\partial y} - \chi n \frac{\partial c}{\partial y} = 0, \quad \text{at } y = 0, 1, \quad 0 \leq x \leq 1,$$

with

$$n(x, y, t_{IC}) \forall x, y = n_{i,j}(\bar{K}_{IC}) \forall i, j,$$
$$e(x, y, t_{IC}) \forall x, y = e_{i,j}(\bar{K}_{IC}) \forall i, j.$$

- As the initial conditions (IC) in the CA are discontinuous, we use the averaged CA simulation results after a short time

# One-Dimensional Model

$$N(x,t) = \int_0^1 n(x,y,t)dy, \quad E(x,t) = \int_0^1 e(x,y,t)dy$$

# Comparison

$$\frac{\partial N}{\partial t} = \boxed{(1 - a_n N - a_e E)} \left[ D \frac{\partial^2 N}{\partial x^2} - \chi \frac{\partial}{\partial x} \left( N \frac{\partial c}{\partial x} \right) \right] - \mu(a_n N^2 + a_e N E) + \lambda c N,$$

$$\frac{\partial E}{\partial t} = \boxed{\mu N + a_n N} \left[ \mu N + D \frac{\partial^2 N}{\partial x^2} - \chi \frac{\partial}{\partial x} \left( N \frac{\partial c}{\partial x} \right) \right],$$

subject to

$$D \frac{\partial N}{\partial x} - \chi N \frac{\partial c}{\partial x} = 0, \quad \text{at } x = 0, 1,$$

$$\frac{\partial N}{\partial t} = D \frac{\partial^2 N}{\partial x^2} - \chi \frac{\partial}{\partial x} \left( N \frac{\partial c}{\partial x} \right) + \lambda N c - \beta_e N E - \beta_n N^2, \quad (\text{A1})$$

$$\frac{\partial E}{\partial t} = \frac{1}{h} \left| D \frac{\partial N}{\partial x} - \chi N \frac{\partial c}{\partial x} \right|, \quad (\text{A2})$$

# Ignored spatial correlations and made mean-field approximations

$$\int_0^1 n^2 dy \approx \left[ \int_0^1 n(x,y,t) dy \right] \times \left[ \int_0^1 n(x,y,t) dy \right]$$
$$\int_0^1 n e dy \approx \left[ \int_0^1 n(x,y,t) dy \right] \times \left[ \int_0^1 e(x,y,t) dy \right]$$

# To summarise

We now have 3 models:

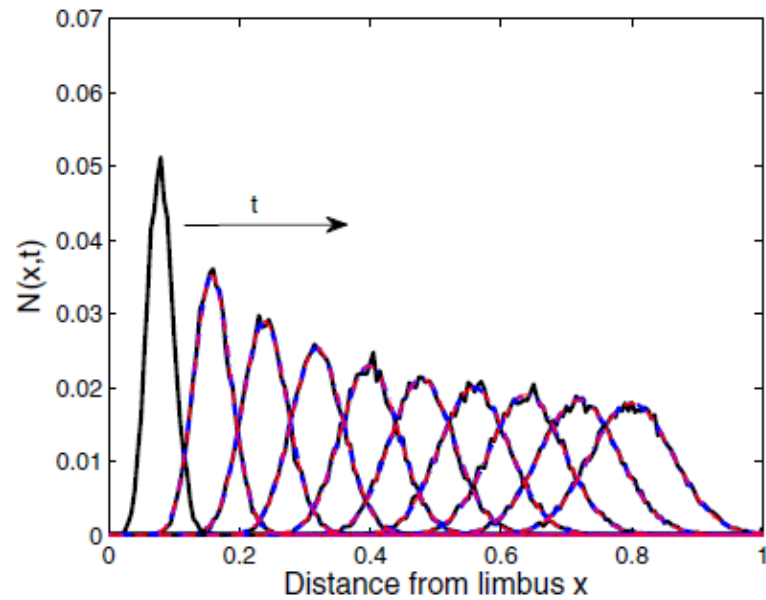
(i) Cellular automaton (true solution) [BLACK]

(ii) Snail-trail (Byrne-Chaplain) continuum model [RED]

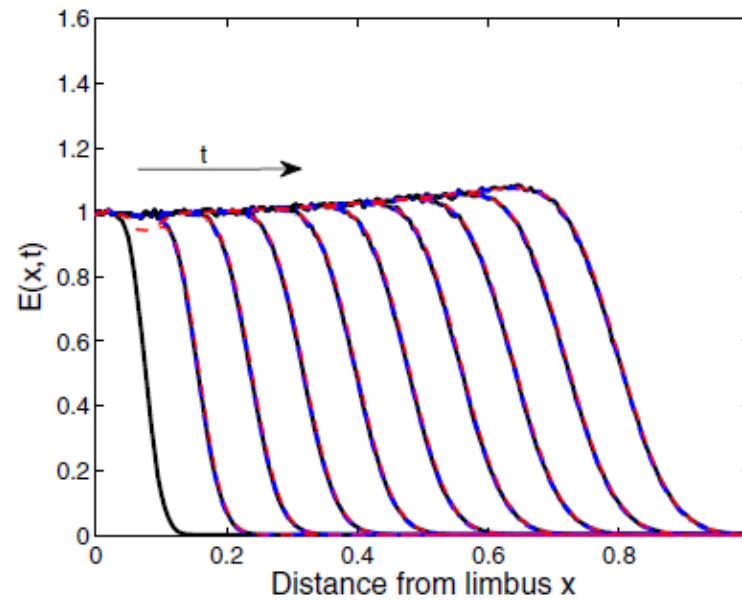
(iii) The new continuum model [BLUE]



# Comparison 1: no anastomosis 😊

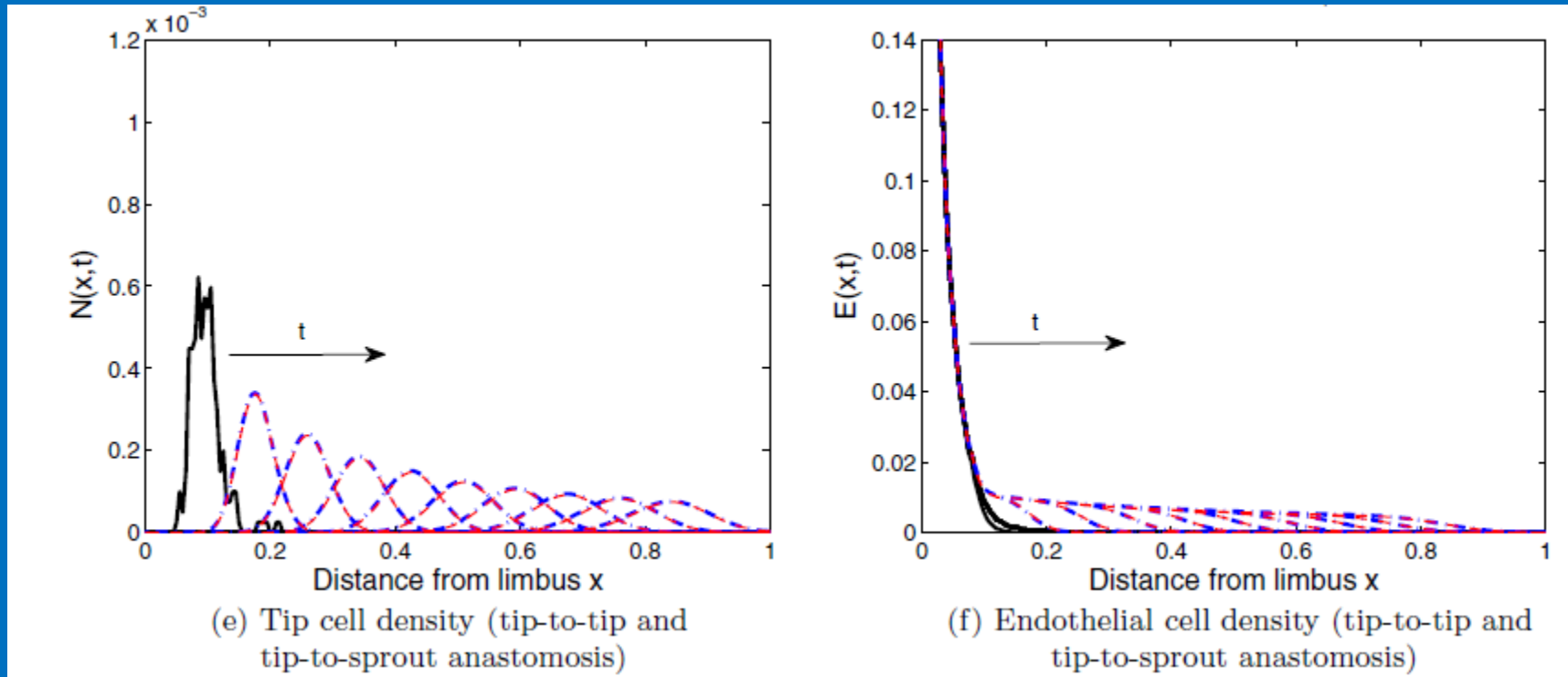


(a) Tip cell density (no anastomosis)



(b) Endothelial cell density (no anastomosis)

# Comparison 2: tip-to-tip and tip-to-sprout anastomoses ☹️



# Summary

- Developed CA model for angiogenesis which has led to a new PDE model for angiogenesis which highlights:
- **(i) Surprisingly, very different looking PDEs give very similar results *for the cases studied***
- **(ii) Mean-field assumption is where things break down**

- W.D. Martinson, H. Ninomiya, H.M. Byrne, P.K. Maini, Comparative analysis of continuum angiogenesis models, *J. Math. Biol.* 82, 2021

# Comparing the models

- We identify two parameter groupings:

$$\varepsilon = \frac{D \lambda}{\chi^2} =$$

(diffusion of tips) x (branching rate)/(chemotaxis coeff)^2

$$\text{and } \alpha = \frac{\lambda}{\mu} =$$

(branching rate)/(tip to tip anastomosis)

If these parameter groupings are small, then a perturbation analysis shows that both models agree to lowest order.

# Comments

- Different models for the same phenomena – how do we systematically compare them?
- How do we coarse-grain from microscale to macroscale?
- How do we relate macroscale parameters to microscale properties?

# **Cancer Cell Invasion**

# Gatenby-Gawlinski Model (1996)

$N_1$  is normal cell density

$N_2$  is tumour cell density

$L$  is lactic acid concentration.

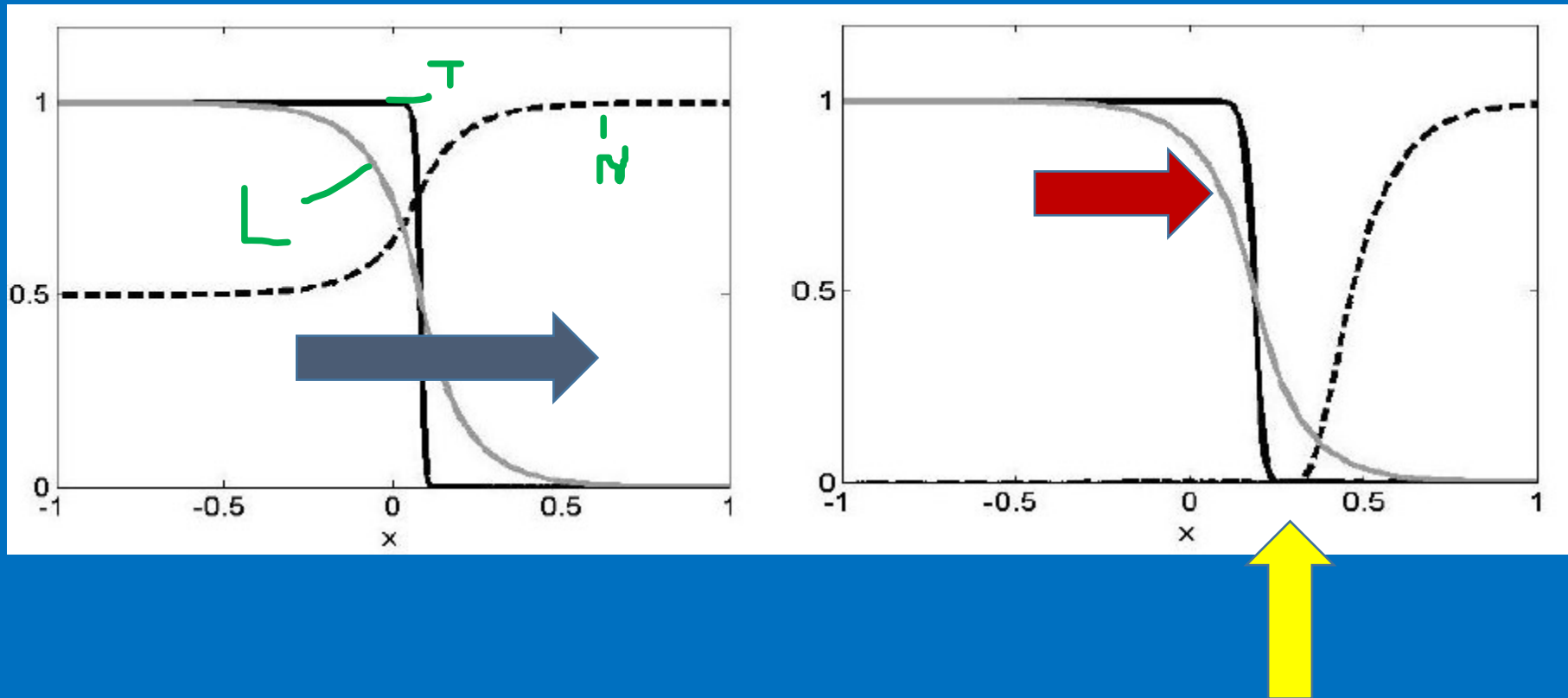
$$\frac{\partial N_1}{\partial t} = r_1 N_1 (1 - N_1/K_1) - d_1 L N_1$$

$$\frac{\partial N_2}{\partial t} = r_2 N_2 (1 - N_2/K_2) + \frac{\partial}{\partial x} [D_2 (1 - N_1/K_1) \frac{\partial N_2}{\partial x}]$$

$$\frac{\partial L}{\partial t} = r_3 N_2 - d_3 L + \frac{\partial^2 L}{\partial x^2}$$

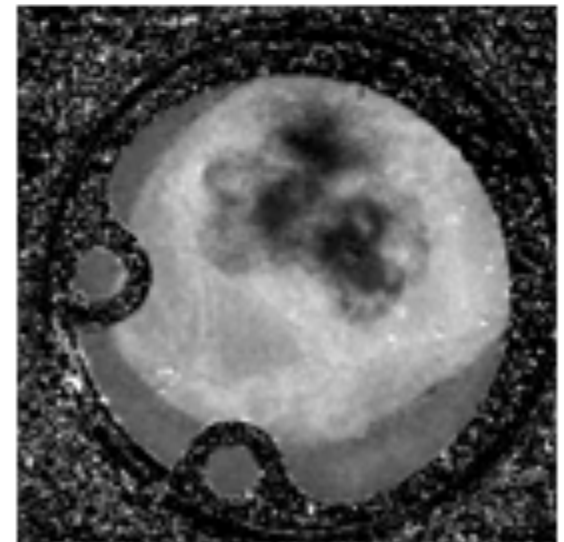
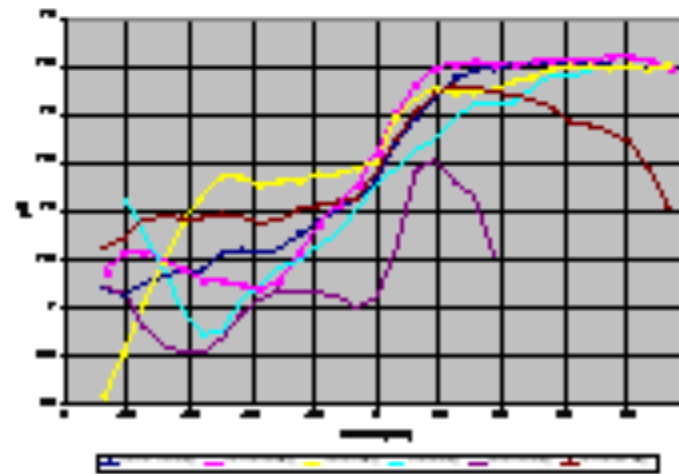
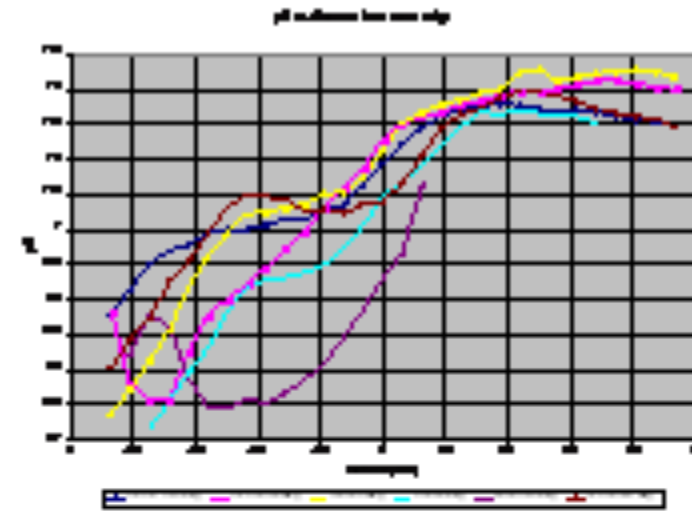
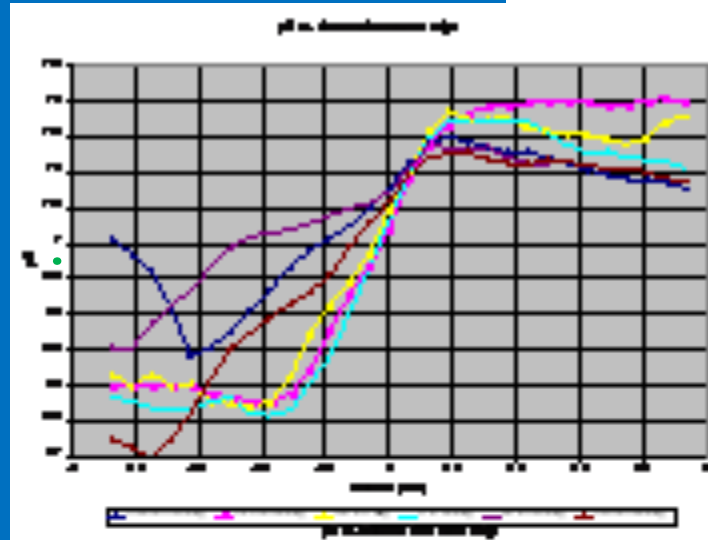
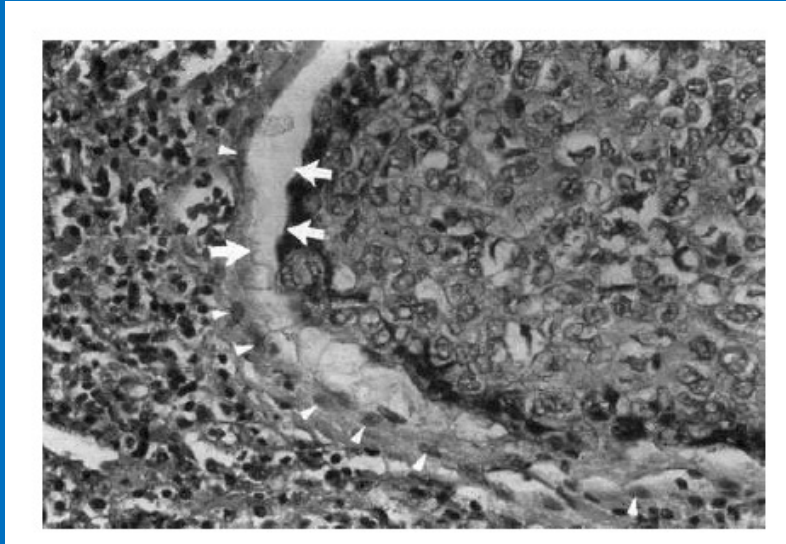
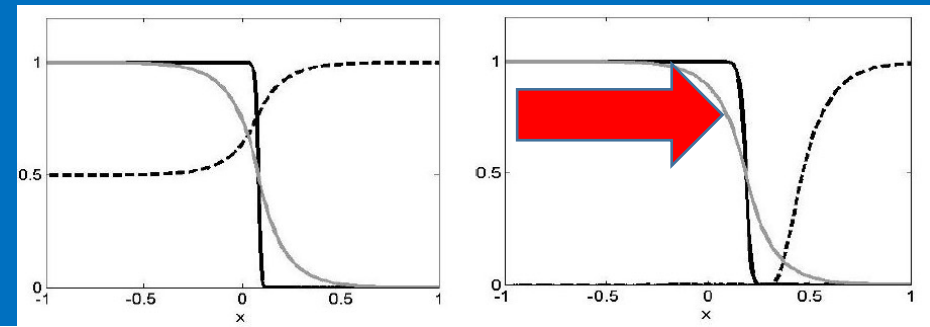


# Travelling waves of invasion



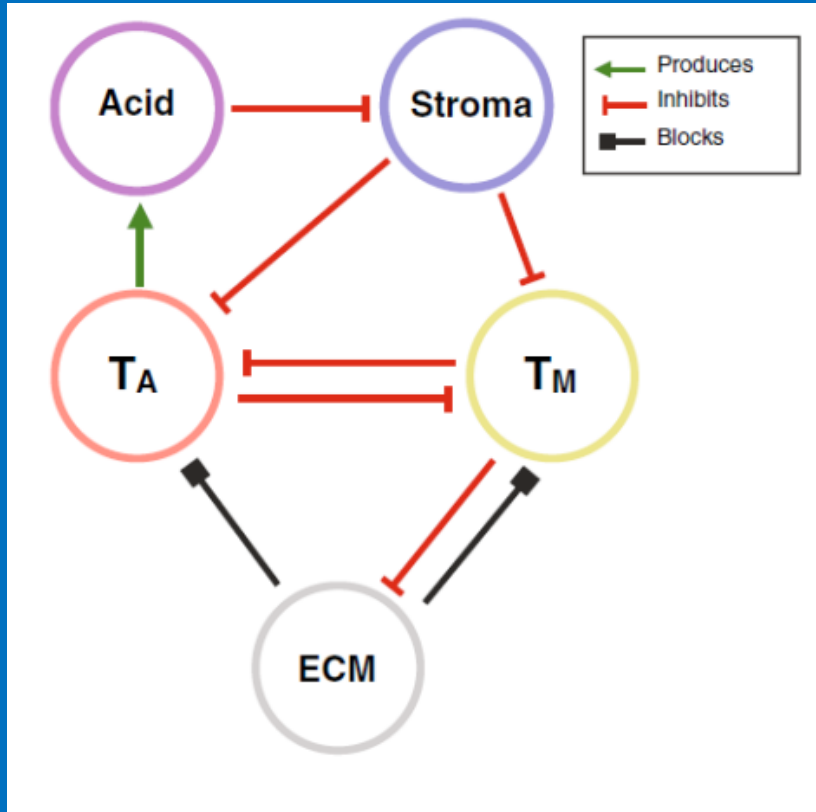
# Experimental results

(Gatenby et al, Cancer Research, 66, 5216-5223, 2006)



M.R.A. Strobl, A.L. Krause, M.Damaghi, R. Gillies, A.R.A. Anderson, P.K. Maini, Mix and Match: phenotypic coexistence as a key facilitator of cancer invasion, B. Math. Biol., 82, 2020

# Co-operation between different cell phenotypes



$$\frac{\partial S}{\partial t} = S(1 - S) - \delta SL,$$

$$\frac{\partial T_A}{\partial t} = \rho_T T_A(1 - c_S S - T_A - c_{M,A} T_M) + \Delta_T \nabla_x \cdot [(1 - M) \nabla_x T_A],$$

$$\frac{\partial T_M}{\partial t} = \rho_T T_M(1 - c_S S - c_{A,M} T_A - T_M) + \Delta_T \nabla_x \cdot [(1 - M) \nabla_x T_M],$$

$$\frac{\partial L}{\partial t} = \rho_L (T_A - L) + \nabla^2 L,$$

$$\frac{\partial M}{\partial t} = -\kappa T_M M,$$

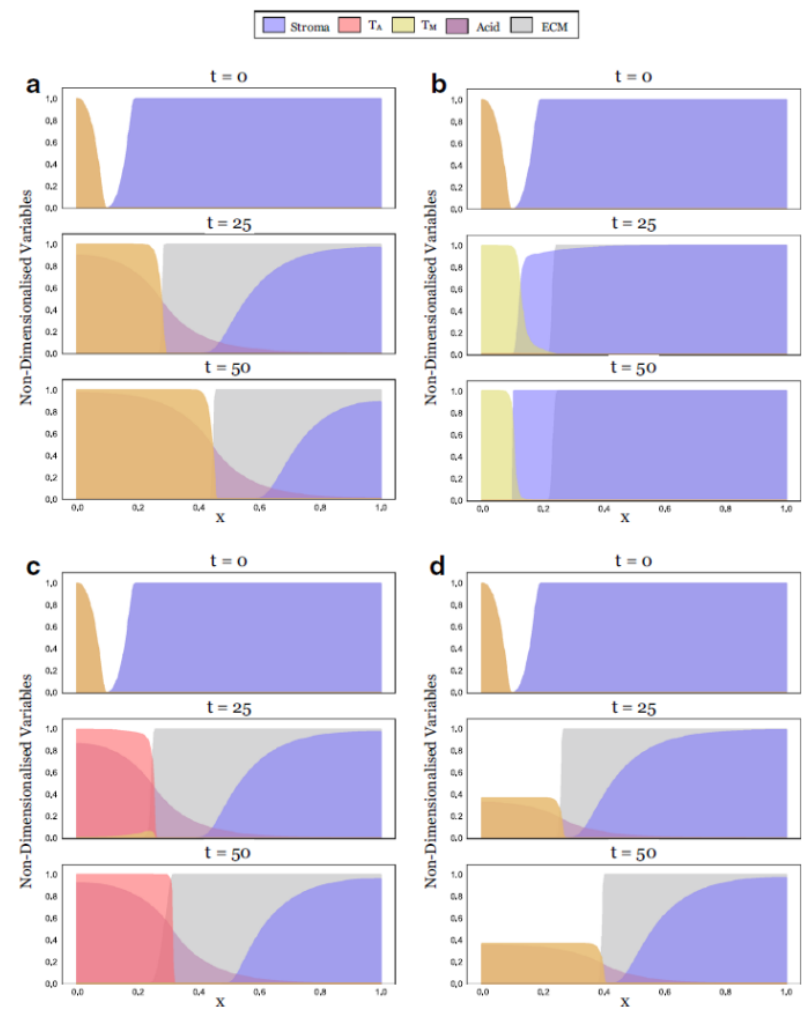


**Fig. 5** Simulations illustrating the four different scenarios that can occur depending on the inter-species competition between  $T_A$  and  $T_M$ . Panels correspond to the locations in the competition parameter space marked in Fig. 4a (1:A, 2:B, 3:C, 4:D). **a**  $(c_{M,A}, c_{A,M}) = (0, 0)$ . At  $t = 0$ , the tumour begins as a mixture of acid-producing (red) and matrix-degrading cells (yellow) on the left-hand side of the domain (appearing orange due to the mixture of the colours). It is constrained by a mixture of stroma (blue) and ECM (grey) on the right-hand side (appearing as dark blue). Since inter-species competition is weak, the tumour populations can coexist and combine their traits, allowing them to invade rapidly ( $t = 25$  and  $t = 50$ ). **b**  $(c_{M,A}, c_{A,M}) = (1.2, 0.7)$ . In contrast, when  $T_M$  dominates over  $T_A$ , it drives  $T_A$  to extinction and no invasion takes place. **c**  $(c_{M,A}, c_{A,M}) = (0.7, 1.2)$ .  $T_A$  dominates over  $T_M$ . While invasion eventually stops due to a lack of ECM degradation, the tumour initially invades thanks to a small population of  $T_M$  persisting at the tumour edge (appearing in orange at  $t = 25$ ). **d**  $(c_{M,A}, c_{A,M}) = (1.7, 1.7)$ . Mutual exclusion of  $T_A$  and  $T_M$ . When seeded at equal densities, the two populations will invade as shown, but the invading front is not stable. If a small perturbation is introduced, the two populations will separate and invasion will halt (Fig. 8)

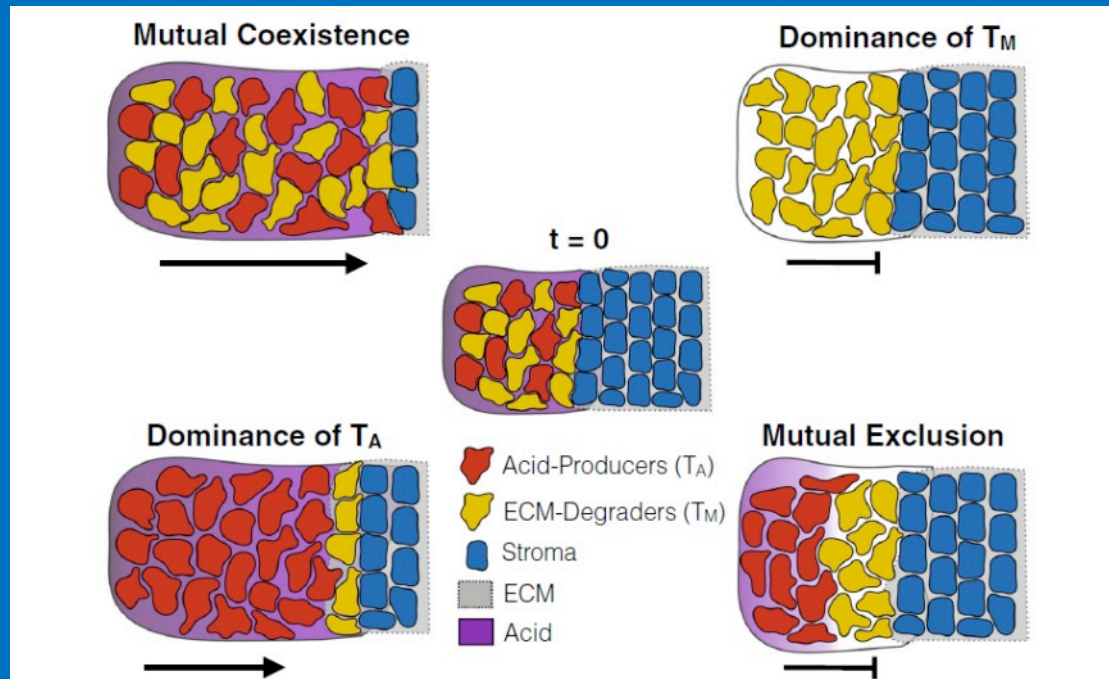


**Fig. 6** Summary of the key findings of this paper. If the two phenotypes can coexist, a highly invasive community of cells emerges. Conversely, if  $T_M$  dominates, tumour invasion comes to a halt as the cells are unable to overcome the stroma. If  $T_A$  dominates, then a temporarily invasive tumour mass forms in which  $T_M$  cells find a temporary habitat in the matrix at the tumour edge. Finally, in the case where the two cell types mutually exclude each other's growth, the cells separate into spatially distinct regions and fail to invade (Colour figure online)

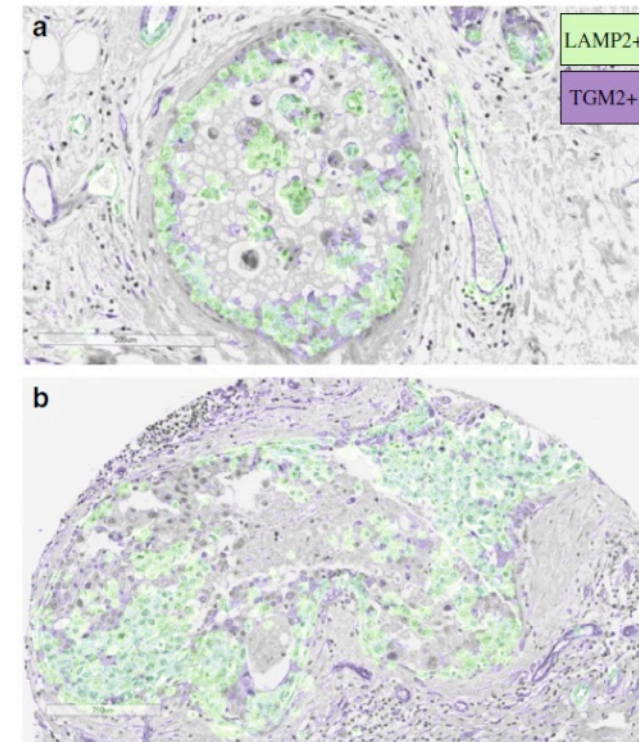


**Fig. 1** Areas of acid production and matrix remodelling in human breast cancer ducts. Acid production was defined by expression of the acid adaptation marker LAMP2 (green). Matrix remodelling was defined by expression of TGM2 (purple). For visualisation purposes, masks were extracted and overlaid on a haematoxylin and eosin stain of the same tissue (see Section A1 for details). **a** Example of a ductal carcinoma in situ that has not yet invaded the surrounding tissue. **b** Example of an invasive cancer that has breached the duct. We observe that not all cells are expressing LAMP2 or TGM2. Could there be cooperation between cells with different traits? (Color figure online)



# Degenerate diffusion really complicates the travelling wave analysis

$$\begin{cases} \frac{\partial N}{\partial t} = \underbrace{\frac{\partial}{\partial x} \left[ D_N \left( 1 - \frac{M}{M_{\text{Max}}} \right) \frac{\partial N}{\partial x} \right]}_{\text{tumour cell movement}} + \underbrace{\rho \left( 1 - \frac{N}{K} \right) N}_{\text{tumour growth}}, \\ \frac{\partial M}{\partial t} = \underbrace{-kMN}_{\text{ECM degradation}}. \end{cases}$$

C. Colson, F. Sánchez-Garduño, H.M. Byrne, P. K. Maini, T. Lorenzi, Travelling-wave analysis of a model of tumour invasion with degenerate, cross-dependent diffusion, Proc. R. Soc. A 477, 20210593 (2021)

Gallay T, Mascia C. 2022 Propagation fronts in a simplified model of tumor growth with degenerate cross-dependent self-diffusivity. *Nonlinear Anal. Real World Appl.* 63, 103387.

# Sketch of Study

$$\begin{cases} \frac{\partial N}{\partial t} = \frac{\partial}{\partial x} \left[ (1 - M) \frac{\partial N}{\partial x} \right] + (1 - N)N, \\ \frac{\partial M}{\partial t} = -\kappa MN. \end{cases} \quad (\text{S0.1})$$

Introducing the travelling wave coordinate  $\xi = x - ct$ , where  $c > 0$ , and the ansatz  $N(x, t) = \mathcal{N}(\xi)$  and  $M(x, t) = \mathcal{M}(\xi)$ , the TWS we seek must satisfy the following ordinary differential equation (ODE) system:

$$\begin{cases} \frac{d}{d\xi} \left( (1 - \mathcal{M}) \frac{d\mathcal{N}}{d\xi} \right) + c \frac{d\mathcal{N}}{d\xi} + (1 - \mathcal{N})\mathcal{N} = 0; \\ c \frac{d\mathcal{M}}{d\xi} - \kappa \mathcal{M}\mathcal{N} = 0, \end{cases} \quad (\text{S0.2a})$$

$$(\text{S0.2b})$$

$$\lim_{\xi \rightarrow -\infty} (\mathcal{N}(\xi), \mathcal{M}(\xi)) = (1, 0), \quad \lim_{\xi \rightarrow +\infty} (\mathcal{N}(\xi), \mathcal{M}(\xi)) = (0, 1), \quad (\text{S0.3})$$

$$\lim_{\xi \rightarrow -\infty} (\mathcal{N}(\xi), \mathcal{M}(\xi)) = (1, 0), \quad \lim_{\xi \rightarrow +\infty} (\mathcal{N}(\xi), \mathcal{M}(\xi)) = (0, \bar{\mathcal{M}}) \text{ with } \bar{\mathcal{M}} \in [0, 1). \quad (\text{S0.4})$$



# Results

- Existence of TWS from  $(1,0)$  to  $(0,1)$  unique for any positive wavespeed (shooting argument).
- For each  $\bar{M} \in [0,1)$  there is a unique TWS from  $(1,0)$  to  $(0, \bar{M})$  for any wavespeed greater than or equal to a strictly positive minimum value.

# Comment

- The inclusion of the simplest nonlinearity in the diffusion term increases the complexity of the analysis of this problem enormously.

**THANK YOU FOR YOUR  
ATTENTION**